

Breast Tumor Recognition by Semantic Segmentation of Multiclass Ultrasound Images

Satish Bansal¹, Rakesh S Jadon², Sanjay K Gupta³

¹Assis. Prof., Dept. of Computer Science and Engineering

Alliance University

Bengaluru, India

e-mail: satish_bansal@rediffmail.com

²Prof., Dept. of Computer Engineering

MITS

Gwalior, India

e-mail: rsjadon@mitsgwalior.in

³Prof., Dept. of SOS in Computer Science & Applications

Jiwaji University

Gwalior, India

e-mail: sanjaygupta9170@gmail.com

Abstract— Objectives: The main purpose of this paper is to suggest a semantic segmentation model to reduce training time in ultrasound breast cancer images. This is achieved by employing a smaller network with fewer trainable parameters, resulting in faster training while maintaining maximum accuracy.

Methods: This paper proposes a modified U-Net model, which we call the V model, for the subdivision of breast tumors. The proposed V architecture is applied explicitly to ultrasound breast cancer datasets for semantic segmentation. Our proposed model achieves semantic segmentation by employing an encoder and decoder on real and mask image datasets.

Findings: Therefore, developing a proposed system, namely a V-Net computer-aided diagnosis (CAD) system, is imperative. This CAD system aims to minimize human errors while enhancing accuracy and speed in the premature finding of breast tumors. The proposed model utilizes minimal layers and parameters while maintaining superior results regarding correctness, speed, and computational proficiency.

Novelty: The proposed V-net model applies to analysing any medical image for detecting disease and finding more accuracy than other U-net models.

Keywords- Ultrasound Image Dataset, CNN, Deep Learning, Breast Cancer. CAD System, mask image, Grayscale Image, V-Net.

1. Introduction

Breast tumors are a substantial root of early mortality among females worldwide. Many medical images, like ultrasound, CT scan and X-ray, are employed for breast cancer analysis. However, conventional and outdated systems often lack effectiveness in diagnosing breast cancer on a global scale. Many artificial intelligence and deep learning algorithms are used for the analysis and detection of breast tumor, but due to poor segmentation analysis, it is complicated to achieve good accuracy. Different authors have developed many computer-aided diagnosis systems (CADs) but only focus on the classification model, not the segmentation process. However, challenges persist in improving the accuracy of CNN models to establish a robust and reliable diagnosis system.

Semantic segmentation is a process in which each pixel is used to classify the image. Semantic segmentation is used to identify breast cancer using the proposed model to improve the segmentation process.

Breast tumors are the second large prevalent malignancy in women [1]. The American Cancer Society declared that breast tumor mortality will rise in the USA. Recently, traditional and advanced technologies, such as the CNN model have been developed for breast tumor detection in mammography [2, 3].

Several authors have previously employed CNNs for mammography segmentation and object detection. Various deep-learning models have been developed on mammography datasets to categorize breast cancer [4-7].

Computer vision analyses, segments, and classifies images in various domains like detection and object recognition in medical pictures. Image segmentation, the procedure of logically separating an image for analysis, has long been employed in these areas. Advanced technologies such as deep learning networks, a subset of artificial intelligence (AI), have emerged, offering remarkable semantic and instance segmentation results.

Segmentation is a complex task that surpasses classification. Humans can perform image segmentation even without prior knowledge of the objects present. Segmentation is crucial for further investigation in medical images, where numerous unknown objects may exist.

Breast cancer detection is mainly applied in X-rays, MRIs and ultrasounds. Segmentation of these images is essential before classification to achieve optimal results. Image segmentation, an established technique, is utilized in image categorization, object recognition, and video analysis. Semantic segmentation, a new technique in deep learning, classifies each pixel as belonging to a specific object, enabling the identification of multiple objects within an image.

Medical image segmentation is often tricky, and FCNs need to improve their spatial resolution when dealing with small objects and irregular image datasets, resulting in deprived segmentation accuracy. To resolve this limitation, the author proposed a new model named U-Net [8-9].

U-NET combines the functions of the decoder and encoder. It facilitates data integration through hop links. This architecture has proven effective in various medical applications, especially mammography. The authors [10] used the finite element segmentation model for one-step segmentation of breast masses, achieving a dice segmentation score of 90.5% in IN-breast databases.

Likewise, the authors [11] developed a method to segment mass lesions in mammography and used film-based digital images and fully digital MG images to estimate the average DICE score. 95.1%, and an average IOU score of 90.9% was achieved.

Current papers highlight the automatic classification of ultrasound breast cancer datasets to help doctors in further treatment using the U-Net model [12]. Different models, algorithms and medical images of breast cancer may modify findings [13].

The trial was conducted on the Breast Mammography Film database. The author developed an algorithm for breast cancer classification from scratch [14], which recovers the skill to distinguish between normal and abnormal breast skin. The author [15] found that there are no better techniques for classification due to many reasons like small datasets, improper segmentation and feature extraction. They developed a pretrained model with a reformed gray wolf optimization algorithm.

The author [16] experimented using a CNN to test breast tumors. Diagnostic performance was evaluated in two mammography databases, DDSM-400 and CBIS-DDSM.

Paper [17] proposed a deep neural network (DNN) imaging method using deep processing techniques and DNN. This method can extract semantic objects and corresponding edges that are good for DNN-based segmentation. The authors [18]

proposed a semantic two-way communication network and a discriminant SDBF network for 3D semantic satellite image recognition from different types of modules.

Researchers [19] projected a method compatible with the original image data. This method improves the image quality as well as the accuracy of each object by semantic segmentation.

To expand the performance level of the segmentation process and classification, a proposed algorithm is required to detect multistage breast cancer on ultrasound images [20].

2. Proposed Methodology:

The dataset [21] was separated into some labels to facilitate image analysis: normal, benign, and malignant. Each class encompasses two categories: 1) a real grayscale image dataset and 2) a mask image dataset. The dataset comprises 1578 images, with a standard size of 500x500 pixels. For compatibility with the proposed model, the resized images to 224X224 pixels.

Figure 1 illustrates the graphical representation of the dataset, depicting an equal distribution of real and mask images among the three labels: Benign, Malignant, and Normal. Figure 2 shows randomly selected samples of real and mask images from the dataset, visually representing the data. Before experimenting, the training, validation, and testing datasets undergo a normalization process.

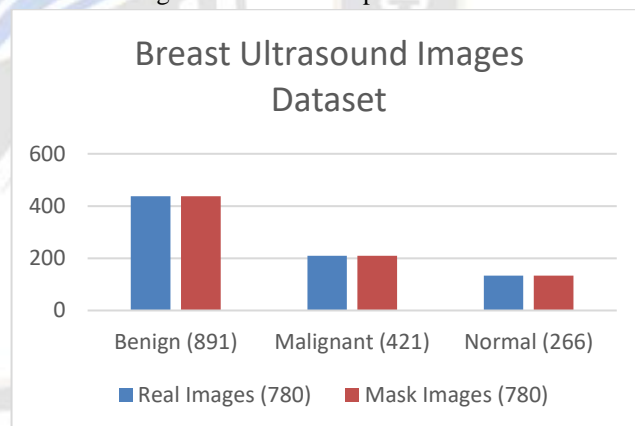


Fig. 1: Images Dataset

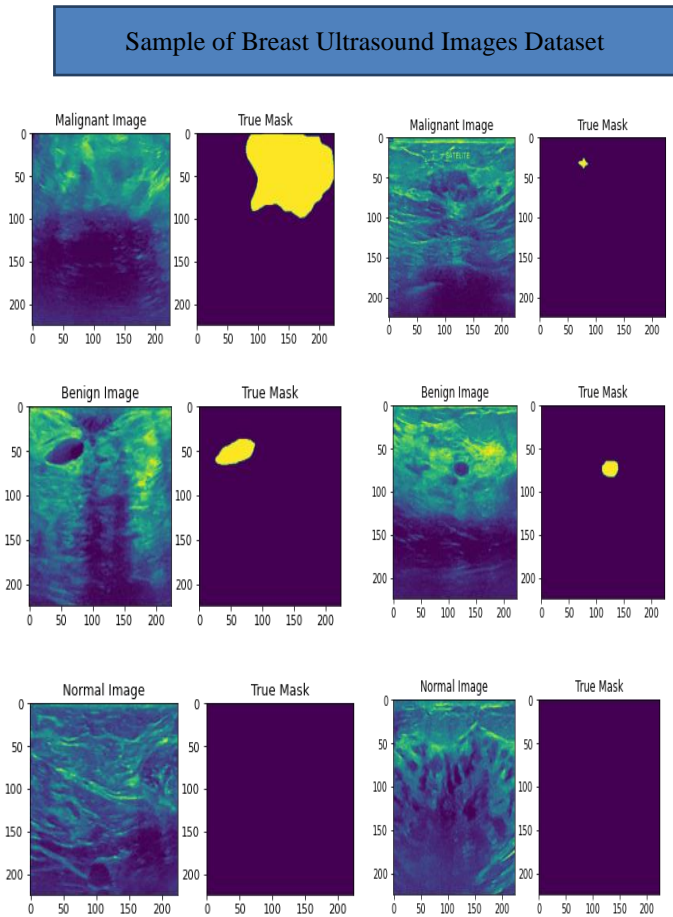


Fig. 2: Sample of Ultrasound Images

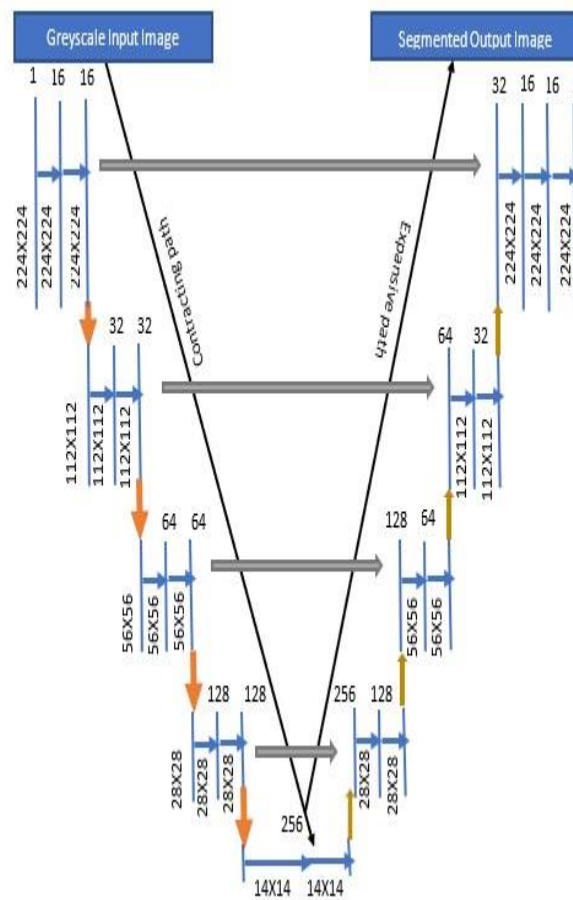


Fig. 3: Architecture of the V-Net Model

Artificial Intelligence (AI) represents the cutting-edge technology employed in various fields. In this study, the V-Net architecture is established explicitly for the semantic segmentation of the ultrasound dataset. The V-Net model exhibits a symmetric architecture that resembles a V shape. The V-Net architecture comprises an encoder path and a decoder path, each serving distinct purposes in semantic segmentation. The down-sampling path utilizes a contracting mechanism, while the up-sampling path employs an expansive mechanism to achieve semantic segmentation.

Figure 3 shows the construction of the V-Net model, in which the image dataset consists of real and mask images. The proposed model used common steps for semantic segmentation like input layer, convolutional, ReLU, pooling and dropout layer. The combinations of diverse layers in the V-net model are used to make the robust model that controls the dataset's overfitting and bias. The proposed model utilizes the different Python 3.6 packages and other necessary libraries. In this experiment, the encoder and decoder paths of a segmented model are depicted in Figures 4 and 5, respectively.

Layer (type)	Output Shape	Param#	Connected to
Model: "functional_1"			
input_1(InputLayer)	(None, 224, 224, 1)	0	
conv2d(Conv2D)	(None, 224, 224, 16)	160	input_1[0][0]
re_lu(ReLU)	(None, 224, 224, 16)	0	conv2d[0][0]
dropout(Dropout)	(None, 224, 224, 16)	0	re_lu[0][0]
conv2d_1(Conv2D)	(None, 224, 224, 16)	2320	dropout[0][0]
re_lu_1(ReLU)	(None, 224, 224, 16)	0	conv2d_1[0][0]
max_pooling2d(MaxPooling2D)	(None, 112, 112, 16)	0	re_lu_1[0][0]
conv2d_2(Conv2D)	(None, 112, 112, 32)	4640	max_pooling2d[0][0]
re_lu_2(ReLU)	(None, 112, 112, 32)	0	conv2d_2[0][0]
dropout_1(Dropout)	(None, 112, 112, 32)	0	re_lu_2[0][0]
conv2d_3(Conv2D)	(None, 112, 112, 32)	9248	dropout_1[0][0]
re_lu_3(ReLU)	(None, 112, 112, 32)	0	conv2d_3[0][0]
max_pooling2d_1(MaxPooling2D)	(None, 56, 56, 32)	0	re_lu_3[0][0]
conv2d_4(Conv2D)	(None, 56, 56, 64)	18496	max_pooling2d_1[0][0]
re_lu_4(ReLU)	(None, 56, 56, 64)	0	conv2d_4[0][0]
dropout_2(Dropout)	(None, 56, 56, 64)	0	re_lu_4[0][0]
conv2d_5(Conv2D)	(None, 56, 56, 64)	36928	dropout_2[0][0]
re_lu_5(ReLU)	(None, 56, 56, 64)	0	conv2d_5[0][0]
max_pooling2d_2(MaxPooling2D)	(None, 28, 28, 64)	0	re_lu_5[0][0]
conv2d_6(Conv2D)	(None, 28, 28, 128)	73856	max_pooling2d_2[0][0]
re_lu_6(ReLU)	(None, 28, 28, 128)	0	conv2d_6[0][0]
dropout_3(Dropout)	(None, 28, 28, 128)	0	re_lu_6[0][0]
conv2d_7(Conv2D)	(None, 28, 28, 128)	147584	dropout_3[0][0]
re_lu_7(ReLU)	(None, 28, 28, 128)	0	conv2d_7[0][0]
max_pooling2d_3(MaxPooling2D)	(None, 14, 14, 128)	0	re_lu_7[0][0]
conv2d_8(Conv2D)	(None, 14, 14, 256)	295168	max_pooling2d_3[0][0]
re_lu_8(ReLU)	(None, 14, 14, 256)	0	conv2d_8[0][0]
dropout_4(Dropout)	(None, 14, 14, 256)	0	re_lu_8[0][0]
conv2d_9(Conv2D)	(None, 14, 14, 256)	590080	dropout_4[0][0]
re_lu_9(ReLU)	(None, 14, 14, 256)	0	conv2d_9[0][0]

Fig. 4: Encoder Path

conv2d_transpose(Conv2DTranspose)	(None, 28, 28, 128)	131200	re_lu_9[0][0]
concatenate(Concatenate)	(None, 28, 28, 256)	0	conv2d_transpose[0][0] re_lu_7[0][0]
conv2d_10(Conv2D)	(None, 28, 28, 128)	295040	concatenate[0][0]
re_lu_10(ReLU)	(None, 28, 28, 128)	0	conv2d_10[0][0]
dropout_5(Dropout)	(None, 28, 28, 128)	0	re_lu_10[0][0]
conv2d_11(Conv2D)	(None, 28, 28, 128)	147584	dropout_5[0][0]
re_lu_11(ReLU)	(None, 28, 28, 128)	0	conv2d_11[0][0]
re_lu_12(ReLU)	(None, 28, 28, 128)	0	re_lu_11[0][0]
conv2d_transpose_1(Conv2DTranspose)	(None, 56, 56, 64)	32832	re_lu_12[0][0]
concatenate_1(Concatenate)	(None, 56, 56, 128)	0	conv2d_transpose_1[0][0] re_lu_5[0][0]
conv2d_12(Conv2D)	(None, 56, 56, 64)	73792	concatenate_1[0][0]
re_lu_13(ReLU)	(None, 56, 56, 64)	0	conv2d_12[0][0]
dropout_6(Dropout)	(None, 56, 56, 64)	0	re_lu_13[0][0]
conv2d_13(Conv2D)	(None, 56, 56, 64)	36928	dropout_6[0][0]
re_lu_14(ReLU)	(None, 56, 56, 64)	0	conv2d_13[0][0]
re_lu_15(ReLU)	(None, 56, 56, 64)	0	re_lu_14[0][0]
conv2d_transpose_2(Conv2DTranspose)	(None, 112, 112, 32)	8224	re_lu_15[0][0]
concatenate_2(Concatenate)	(None, 112, 112, 64)	0	conv2d_transpose_2[0][0] re_lu_3[0][0]
conv2d_14(Conv2D)	(None, 112, 112, 32)	18464	concatenate_2[0][0]
re_lu_16(ReLU)	(None, 112, 112, 32)	0	conv2d_14[0][0]
dropout_7(Dropout)	(None, 112, 112, 32)	0	re_lu_16[0][0]
conv2d_15(Conv2D)	(None, 112, 112, 32)	9248	dropout_7[0][0]
re_lu_17(ReLU)	(None, 112, 112, 32)	0	conv2d_15[0][0]
re_lu_18(ReLU)	(None, 112, 112, 32)	0	re_lu_17[0][0]
conv2d_transpose_3(Conv2DTranspose)	(None, 224, 224, 16)	2064	re_lu_18[0][0]
concatenate_3(Concatenate)	(None, 224, 224, 32)	0	conv2d_transpose_3[0][0] re_lu_1[0][0]
conv2d_16(Conv2D)	(None, 224, 224, 16)	4624	concatenate_3[0][0]
re_lu_19(ReLU)	(None, 224, 224, 16)	0	conv2d_16[0][0]
dropout_8(Dropout)	(None, 224, 224, 16)	0	re_lu_19[0][0]
conv2d_17(Conv2D)	(None, 224, 224, 16)	2320	dropout_8[0][0]
re_lu_20(ReLU)	(None, 224, 224, 16)	0	conv2d_17[0][0]
re_lu_21(ReLU)	(None, 224, 224, 16)	0	re_lu_20[0][0]
conv2d_18(Conv2D)	(None, 224, 224, 1)	17	re_lu_21[0][0]
Total params: 1,940,817			
Trainable params: 1,940,817			
Non-trainable params: 0			

Fig. 5: Decoder Path

Different authors have employed various U-Net models for different types of classification. The proposed V-net model utilized a specific configuration comprising fewer layers and parameters, as summarized in Table [1].

Table 1: Comparison of the Segmentation Model

Segmentation Model	V-net Model	U-net Model
Convolutional Layer	18	23
Training Parameter	1,940,817	31,402,501

Many authors have utilized pretrained CNN models comprising various layers such as convolutional, pooling, ReLU, and softMax, with layer sizes increasing accordingly.

However, for the specific problem, the U-net model was modified and transformed into the V-net model, which incorporates compact layers and parameters compared to the U-net construction.

In this study, training options such as a learning rate, batch size and number of epochs are 0.0001, 16 and 100 respectively were considered during the experiment, and it

was determined that the optimal number of training options is suitable for achieving desirable results.

3. Result:

The experimental results are shown in Table 2, which calculates the following matrices for semantic segmentation accuracy, loss, mean squared error (MSE), area under curve (AUC), Dice coefficient (Dice Coeff) and intersection over union (IOU Coeff).

Table 2: Performance Metrics

Proposed V net Segmented Model	Loss	MSE	Accuracy	AUC	Dice Coeff	IOU Coeff
Training Data	0.013	0.003	0.993	0.999	0.946	0.780
Validation Data	0.275	0.040	0.953	0.886	0.630	0.475
Testing data	0.276	0.034	0.960	0.874	0.685	0.465

The performance of a model is crucial in determining its reliability in the field of medical segmentation. The evaluation metrics mentioned previously play a substantial role in assessing the model's performance. These performance metrics are visually shown in a column chart, as depicted in Figure 6 and Figure 7, which shows the training dataset's different measures.

Accuracy is computed by examining each pixel and assigning a score of 1 if the pixel is correctly predicted based on the corresponding mask and 0 otherwise. Mathematically, accuracy can be represented as:

$$\text{Accuracy (A, B)} = \begin{cases} 1 & \text{if } (A_i=B_i), \\ 0 & \text{Otherwise} \end{cases}$$

The accuracies are 99%, 95% and 96% for the training, validation and test data, respectively.

The AUC evaluates the performance of a segmentation net. In this proposed model, the AUC for the training is 99%, validation is 88% and testing is 87%. The high AUC values indicate excellent performance in accurately classifying the data. A higher AUC value signifies better class discrimination and effectively demonstrates the model's measurements can distinguish between classes.

The IOU, also referred to as the Jaccard index and Dice coefficient is considered the most influential metric for evaluating the performance of models in semantic segmentation. The IOU determines the overlay among the predicted value (X) and ground value (Y), divided by the merger of their respective areas.

The IOU coefficients found for the training, validation, and test datasets are 78%, 47%, and 46%, respectively. These values indicate satisfactory performance, demonstrating the model's ability to accurately capture the overlapping regions between the predicted and ground values in each dataset.

$$\text{IOU Coeff} = J(X, Y) = A / (B - C)$$

The Dice coefficient can be defined in both images (real and mask) by using the following equation.

$$\text{Dice_Coeff} = DC(X, Y) = 2 * A / B$$

$$\text{Where } A = |X \cap Y|, B = |X| + |Y|, C = |X \cap Y|$$

The Dice coefficients are 94%, 63% and 68% for the training, validation and test datasets, respectively, which are better than the IOU coefficients.

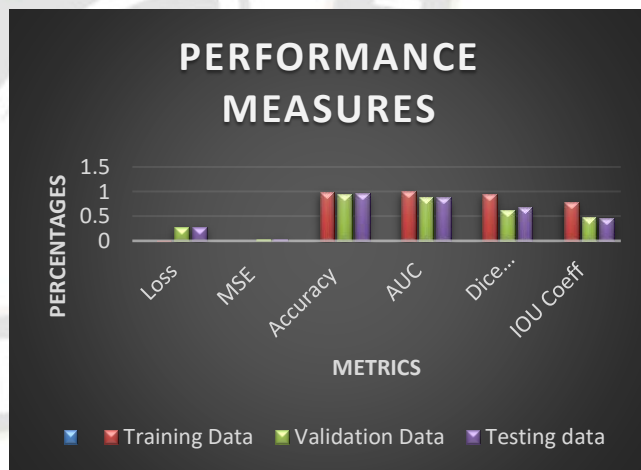


Fig. 6: Performance Chart

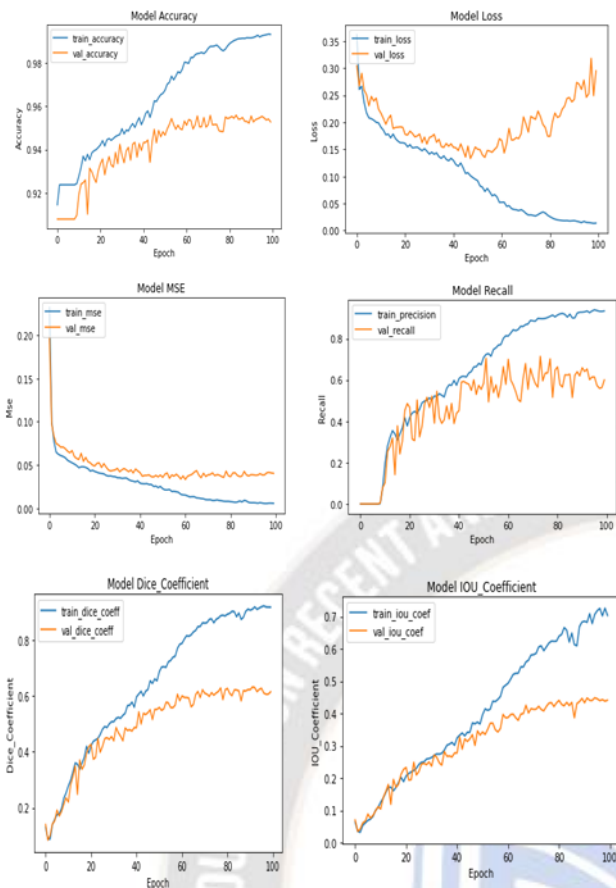


Fig. 7: Training graph of different measures

Figures 8(a), 8(b), 8(c), 8(d) and 8(e) demonstrate the final results of the proposed v-net model on different images. Each sample shows four images starting from the left original mask, predicted mask, process mask and original image of different classes (benign, malignant and normal).

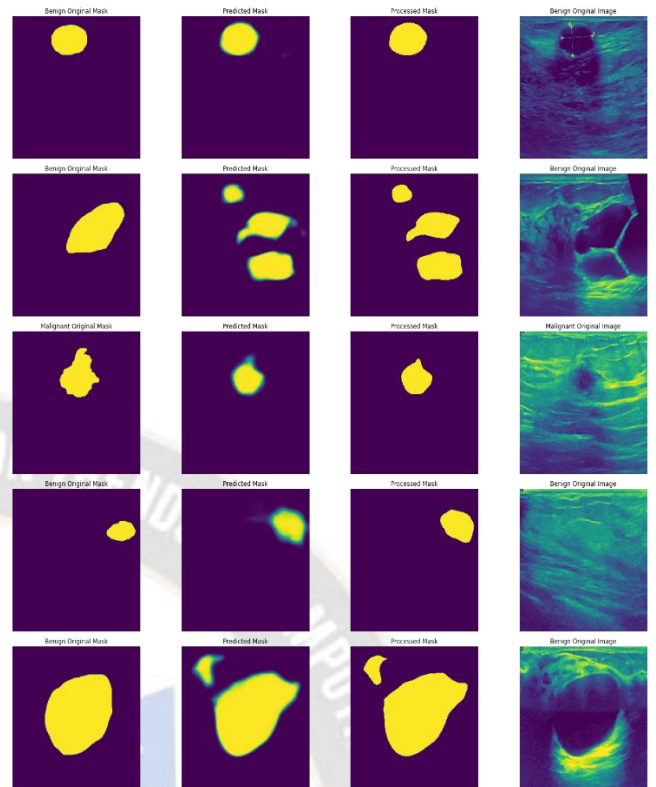


Fig. 8(a): The results of the proposed model

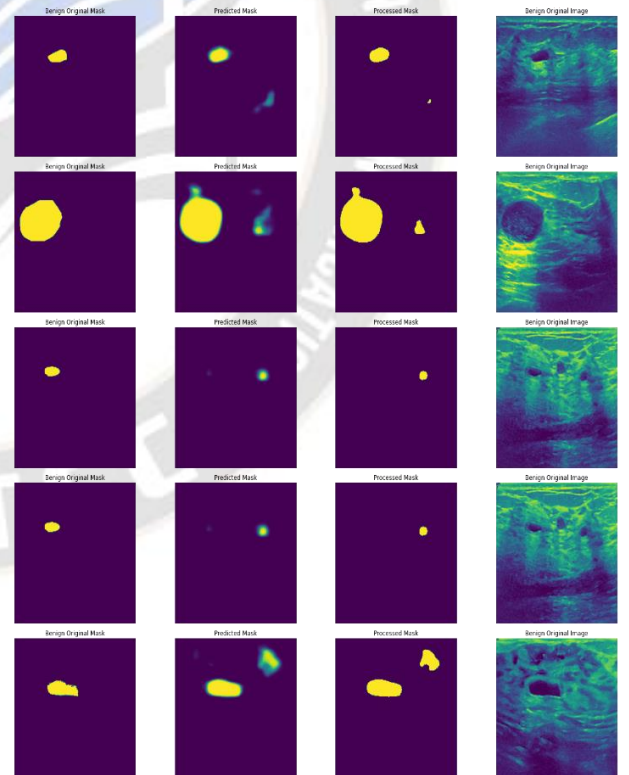


Fig. 8(b): The results of the proposed model

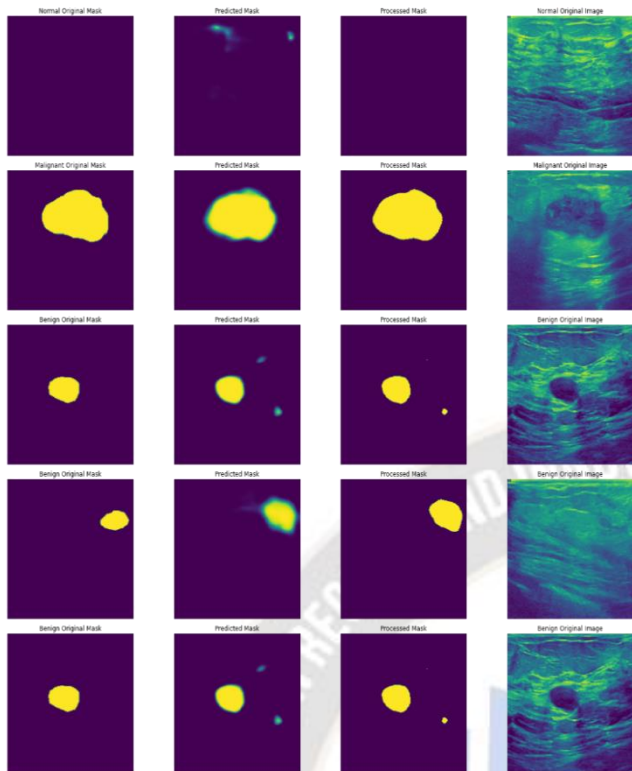


Fig. 8(c): The results of the proposed model

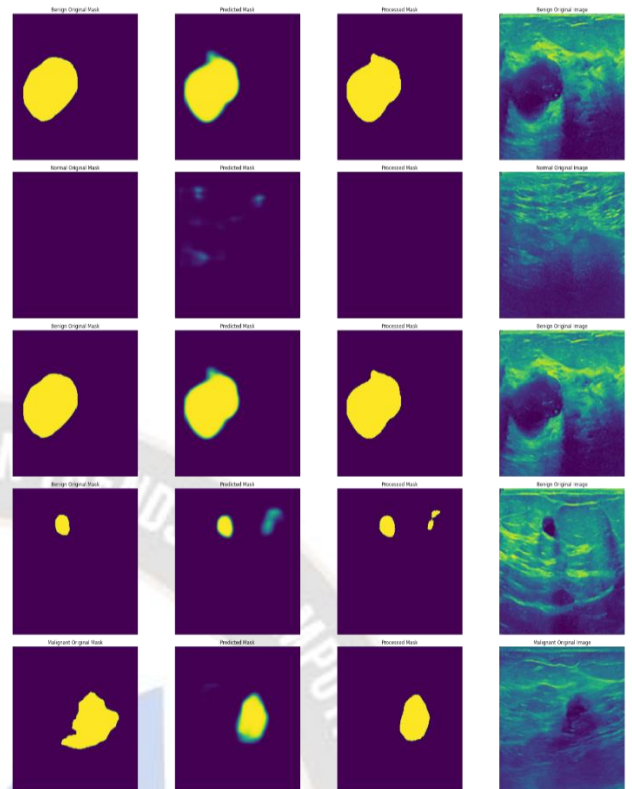


Fig. 8(e): The results of the proposed model

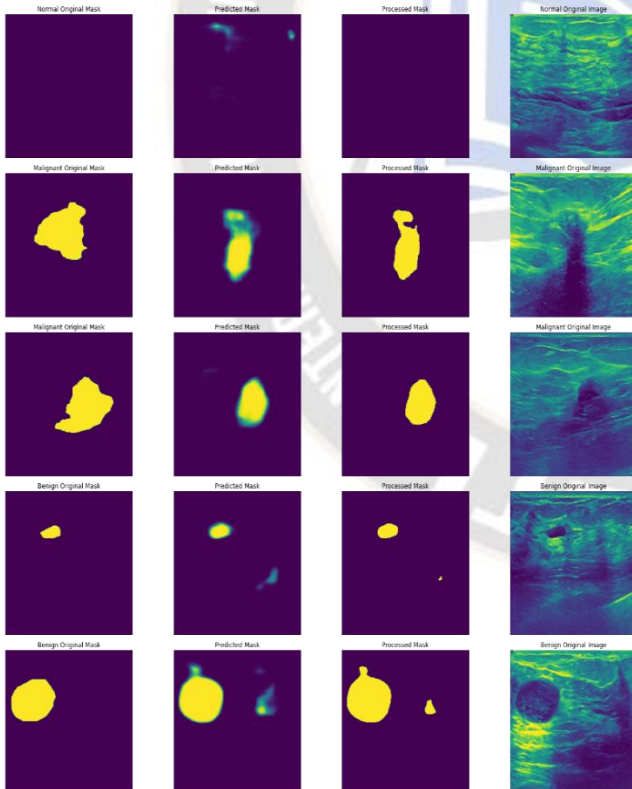


Fig. 8(d): The results of the proposed model

Table 3 compares different segmentation representations with my proposed model, which describes how this planned model is improved over other models.

Table 3: Comparison of the proposed model with other models

Methods	Accuracy	Dice	IOU Coeff
Attention Unet [22]	96.45%	78.77%	69.99%
Deeplabv3+ [22]	96.67%	80.12%	70.34%
Proposed V-net	99.3%	94.6%	78%

4. Conclusions:

The scientific evidence presented in this study validates the effectiveness of detecting breast cancer and classifying breast ultrasound images using both real and mask datasets. The mask images, representing segmented images, demonstrate advantages such as reduced classification time and improved accuracy.

The proposed semantic segmentation model, V-net, incorporates modifications to the U-NET model specifically for breast cancer diagnosis. The model's performance is estimated based on metrics such as accuracy, intersection-over-union (IOU), area under curve (AUC), and Dice coefficient (DC).

Semantic segmentation techniques have demonstrated their superiority and efficiency compared to traditional segmentation models. This method holds significant applications in medical image processing and computer vision.

The primary focus of this paper is on the advancements made in the semantic segmentation of ultrasound images. Furthermore, in future instances segmentation can also be performed on medical images, contributing to enhanced accuracy in diagnosis. Hybrid models, which are combinations of deep learning and optimization algorithms or fuzzy logic, can also be used to increase accuracy with consistency.

Competing Interests: No conflicts of interest

Funding: No funding from any source.

Acknowledgements: I'd like to thank my guides.

Authors Contribution: Conceptual study, collection of data and experiment done by me. Writing review, analysis and methodology done by my guides.

References:

1. Feiqian W, Xiaotong L, Buyue Q, Litao R, Rongjian Z, Changchang Y, et al. Spatial Attention Lesion Detection on Automated Breast Ultrasound. In: Bioinformatics and Biomedical Engineering. 7th International Work-Conference, IWBBIO 2019, 8-10 May 2019. vol. pt. I of Bioinformatics and Biomedical Engineering. 7th International Work-Conference, IWBBIO 2019. Proceedings: Lecture Notes in Bioinformatics (LNBI 11465). Springer International Publishing;. p. 216–27. http://dx.doi.org/10.1007/978-3-030-17938-0_20.
2. Zhang, S.-C.; Hu, Z.-Q.; Long, J.-H.; Zhu, G.-M.; Wang, Y.; Jia, Y.; Zhou, J.; Ouyang, Y.; Zeng, Z. Clinical implications of tumor-infiltrating immune cells in breast cancer. *J. Cancer* 2019, 10, 6175. [CrossRef] [PubMed].
3. Abdelhafiz D, Yang C, Ammar R, Nabavi S. Deep convolutional neural networks for mammography: advances, challenges and applications. *BMC Bioinformatics*. 2019;20(11):281.
4. Giacomello, E., Loiacono, D. & Mainardi, L. Brain MRI tumor segmentation with adversarial networks. In 2020 International Joint Conference on Neural Networks (IJCNN), 1–8 (IEEE, 2020).
5. Henriksen, E. L., Carlsen, J. F., Vejborg, I. M., Nielsen, M. B. & Lauridsen, C. A. The efficacy of using computer-aided detection (CAD) for detection of breast cancer in mammography screening: a systematic review. *Acta Radiol*. 60, 13–18 (2019).
6. Mulooly, M. et al. Application of convolutional neural networks to breast biopsies to delineate tissue correlates of mammographic breast density. *npj Breast Cancer* 5, 1–11 (2019).
7. Singh, V. K. et al. Breast tumor segmentation and shape classification in mammograms using generative adversarial and convolutional neural network. *Expert Syst. Appl.* 139, 112855 (2020).
8. Du G, Cao X, Liang J, Chen X, Zhan Y. Medical image segmentation based on U-Net: A review. *Journal of Imaging Science and Technology*. 2020; 64(2). <https://doi.org/10.2352/J.ImagingSci.Technol.2020.64.2.020508>.
9. Wang, Y., Yao, Y., 2022. Breast lesion detection using an anchor-free network from ultrasound images with segmentation-based enhancement. *Sci. Rep.* 12, 1–11. <https://doi.org/10.1038/s41598-022-18747-y>.
10. Soulam, K. B., Kaabouch, N., Saidi, M. N. & Tantaoui, A. Breast cancer: one-stage automated detection, segmentation, and classification of digital mammograms using UNet model based-semantic segmentation. *Biomed. Signal Process. Control* 66, 102481 (2021).
11. Abdelhafiz, D., Bi, J., Ammar, R., Yang, C. & Nabavi, S. Convolutional neural network for automated mass segmentation in mammography. *BMC Bioinformatics* 21, 1–19 (2020).
12. : Guo Y, Duan X, Wang C, Guo H (2021) Segmentation and recognition of breast ultrasound images based on an expanded U-Net. *PLoS ONE* 16(6): e0253202. <https://doi.org/10.1371/journal.pone.0253202>.
13. Shia, W.-C.; Hsu, F.-R.; Dai, S.-T.; Guo, S.-L.; Chen, D.-R. Semantic Segmentation of the Malignant Breast Imaging Reporting and Data System Lexicon on Breast Ultrasound Images by Using DeepLab v3+. *Sensors* 2022, 22, 5352. <https://doi.org/10.3390/s22145352>.
14. L. Tsochatzidis, L. Costaridou, I. Pratikakis, Deep learning for breast cancer diagnosis from mammograms—a comparative study, *J. Imaging* 5 (3) (2019) 37.
15. Jabeen, K.; Khan, M.A.; Alhaisoni, M.; Tariq, U.; Zhang, Y.-D.; Hamza, A.; Mickus, A.; Damaševičius, R. Breast Cancer Classification from Ultrasound Images Using Probability-Based Optimal Deep Learning Feature Fusion. *Sensors* 2022, 22, 807. <https://doi.org/10.3390/s22030807>.
16. L. Tsochatzidis, P. Koutla, L. Costaridou, and I. Pratikakis, “Integrating segmentation information into CNN for breast cancer diagnosis of mammographic masses,” *Computer Methods and Programs in Biomedicine*, vol. 200, p. 105913, 2021.
17. J. Hong-Gu, J. Hyeon-Woo, Y. Byung-Hyun, and C. KangSun, “Image segmentation algorithm for semantic segmentation with sharp boundaries using image processing and deep neural network,” *IEEE International Conference on Consumer Electronics - Asia*, p. 4, 2020.
18. Z. Rao, M. He, Z. Zhu, Y. Dai, and R. He, “SDBF-net: semantic and disparity bidirectional fusion network for 3D semantic detection on incidental satellite images,” in *Proceeding of the Annual Summit and Conference of the Asia-Pacific-Signal and Information-Processing-Association (APSIPA ASC)*, pp. 438–444, Lanzhou, November 2019.
19. D. W. Yang, Y. Du, H. Yao, and L. Bao, “Image semantic segmentation with hierarchical feature fusion based on deep neural network,” *Connection Science*, vol. 34, no. 1, pp. 1772–1784, 2022.

20. Se Woon Cho, Na Rae Baek, Kang Ryoung Park, Deep Learning-based Multi-stage segmentation method using ultrasound images for breast cancer diagnosis, Journal of King Saud University - Computer and Information Sciences, Volume 34, Issue 10, Part B, 2022, Pages 10273-10292, <https://doi.org/10.1016/j.jksuci.2022.10.020>.
21. Dataset is available on <https://www.kaggle.com/datasets/aryashah2k/breast-ultrasound-images-dataset>.

